Inorganic Chemistry

Article

pubs.acs.org/IC

Role of Ruthenium Oxidation States in Ligand-to-Ligand Charge Transfer Processes

Cristina L. Ramírez,[†] César N. Pegoraro,[†] Oscar Filevich,[‡] Andrea Bruttomeso,[§] Roberto Etchenique,[‡] and Alejandro R. Parise*[,†]

[†]Departamento de Química, FCEN−Universidad Nacional de Mar del Plata, Funes 3350, 7600 Mar del Plata, Argentina

[‡]INQUIMAE−Departamento de Química Inorgánica, Analítica y Fisicoquímica and [§]Departamento de Química Orgánica, FCEN−Universidad de Buenos Aires, Ciudad Universitaria, 1428 Buenos Aires, Argentina

Supporting Information

ABSTRACT: We describe in this paper the properties of $[Ru^{II/III}(bpy)_2ClL]^{+1/+2}$ and $[Ru^{II/III}(bpy)_2L_2]^{+2/+3}$. L = ditolyl-3-pyridylamine (**dt3pya**) is a redox active ligand related to triarylamines, which is very similar to 3-aminopyridine except for the reversible redox behavior. The monosubstituted complex shows a metal-to-ligand charge-transfer (MLCT) at 502 nm, and reversible waves in acetonitrile at $E^0(Ru^{III/II})$ = 1.07 V, $E^0(L^{+/0})$ = 1.46 V (NHE). The disubstituted complex shows an MLCT at 461 nm, a photorelease of **dt3pya** with quantum yield of 0.11 at 473 nm, and two reversible one-electron overlapped waves at 1.39 V associated with one of the ligands (1.37 V) and $Ru^{III/II}$ (1.41 V). Further oxidation of the second ligand at 1.80 V forms a 2,2′-bipiridine derivative, in an irreversible reaction similar to dimerization of triphenylamine to yield tetraphenylbenzidine. In the dioxidized state, the spectroelectrochemistry of the disubstituted complex shows a ligand-to-ligand charge transfer at 1425 nm, with a transition moment of 1.25 Å and an effective two-state coupling of 1200 cm^{-1}. No charge transfer between ligands was observed when Ru was in a 2+ oxidation state. We propose that a superexchange process would be involved in ligand−metal−ligand charge transfer, when ligands and metals are engaged in complementary π interactions, as in metal−ligand−metal complexes. Best orbital matching occurs when metallic donor fragments are combined with acceptor ligands and vice versa. In our case, Ru^{III} bridge (an acceptor) and two **dt3pya** (donors, one of them being oxidized) made the complex a Robin−Day Class II system, while the Ru^{II} bridge (a donor, reduced) was not able to couple two **dt3pya** (also donors, one oxidized).

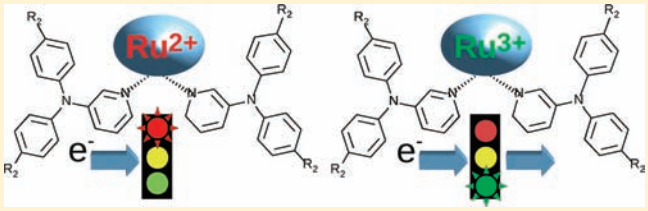

INTRODUCTION

Mixed-valence compounds have played a central role in the understanding of how electron transfer occurs in a variety of systems whose properties (color, electrical conductivity, magnetism) derive from this phenomenon. This topic has been systematized in a series of reviews,[1−10] and its influence on the field of electron transfer has been so strong that we are currently able to trace applications of the intervalence concept in fields so apparently unconnected as magnetoresistance,[11] energy conversion,[12] and molecular electronics.[13] The most important strength of intervalence compounds, such as the Creutz-Taube cation, is that they allow us to spectroscopically interrogate the system that actually performs the electron transfer event. This observation is not possible while studying homogeneous redox reactions like solution self-exchange $Fe(H_2O)_6^{2+}/Fe(H_2O)_6^{3+}$ (a classic example), because reacting ions are nonassociated most of the time and spectroscopies are usually not sensitive enough to allow studying the small concentration of associated reactants.

Although ligands are usually organic molecules, and organic mixed valence systems have made important contributions to this field,[14] ligand-focused charge transfer and ligand−metal−ligand mixed valence compounds are notoriously scarce in electron transfer literature.[15] The set of compounds studied so far is small because most redox-active ligands are also involved in coupled irreversible chemical reactions that hinder molecular interrogation (usually formation of multiple N−C bonds accompanied by proton transfer after the electrochemical step[16]). The analysis of these systems focused on ligand charge transfer should not differ essentially from the classical metal−ligand−metal system like the Creutz-Taube cation, because the underlying electron transfer theory is independent of the nature of the fragments involved in redox reactions.

It has been proposed[15] that a pure ligand−ligand charge transfer (a concept analogous to a metal−metal intervalence charge transfer) must have no influence of the central metal. In this extreme situation, the metal locates the ligands in such a way that direct orbital overlapping results in electronic coupling. In other words, the metal has a structural connectivity role but not an electronic (orbital) role. On the basis of the experience of the historically metal-focused mixed valence chemistry, this extreme situation of negligible coupling between adjacent metal−ligand pairs and non-negligible coupling

Received: May 9, 2011
Published: January 6, 2012

   dx.doi.org/10.1021/ic200966f | *Inorg. Chem.* 2012, 51, 1261−1268

between remote metals seems to be rather the exception than the rule. Even in metal localized mixed-valence compounds like $[Ru(NH_3)_5$-4,4′-bipyridine-$Ru(NH_3)_5]^{5+}$ there is always some kind of interaction with the bridge, reflected in the appearance of a metal-to-ligand charge-transfer (MLCT) beside a metal-to-metal charge transfer (MMCT). In these cases, the interactions between adjacent sites are responsible for an electron transfer process involving remote metals, without a direct metal−metal coupling (a superexchange bridge-mediated mechanism).

Here, we will describe the mono and dicoordination of ditolyl-3-pyridylamine, which is a redox-active arylamine derivative, into the fragment $[Ru^{III/II}(bpy)_2]^{3+/2+}$ (bpy is 2,2′-bipyridine). The family of coordination compounds derived from $[Ru^{II}(bpy)_3]^{2+}$ has been widely studied for their photochemical properties, especially the charge transfer capability from the excited electronic states.[17] Because of this characteristic, the chemistry of these compounds has shown to be attractive because of its potential application in systems for turning visible radiation into chemical energy,[18,19] a topic that has become a priority because of the new social values regarding the use of natural resources. In this direction, the use of the fragment $[Ru^{II}(bpy)(SCN)_2]^0$ with bidentate ligands derived from triarylamines (redox-active) that allows a fast in situ regeneration of the Ru^{III} fragment formed after charge injection into the supporting semiconductor has been recently reported.[20] Triarylamines are a family of compounds which has received considerable attention in recent years as hole transport materials, because of their chemical robustness and versatility in derivatization for controlling their redox potential.[21] Since their E^0 is close to that of the $[Ru^{III/II}(bpy)_x]^{+3/+2}$ series, these fragments are interesting to be incorporated in redox optoelectronic devices for electrical conduction.

EXPERIMENTAL SECTION

Reagents and solvents were purchased from Sigma-Aldrich, Anedra, Dorwill, and Cicarelli. Solvents were purified as described elsewhere.[22] $[Ru(bpy)_2Cl_2]^0$ and $[Ru(bpy)_2(3\text{-aminopyridine})_2](PF_6)_2$ were synthesized as previously described.[23,24] Electrochemical experiments were measured in an anaerobic three-electrode cell with a silver wire as a pseudoreference, a 50 μ platinum disk as working electrode, and a platinum wire as a counterelectrode. Redox potentials were reported against NHE (ferrocene was added as internal standard after measurements[25]). Spectroelectrochemistry experiments were performed with a four-electrode quartz thin layer cell using a graphite felt counterelectrode, platinum woven wire working electrode (70 μ wires), a silver pseudoreference and an additional small platinum electrode to measure cyclic voltammograms prior to the electrolysis. Electronic spectra were measured in a Shimadzu spectrophotometer UV-3101PC, electrochemistry experiments with a potentiostat TEQ-3, NMR spectra in a Bruker AM-500, and high resolution mass spectra in a Bruker micrOTOF-QII.

The setup to measure the photolysis quantum efficiencies consisted of three collinearly aligned lasers at 532 nm, 473 nm, and 405 nm respectively. An Ocean Optics PC2000 diode-array spectrophotometer was mounted normally to the laser light path as in a fluorescence setup. A quartz cuvette was at the center of the arrangement in an aluminum holder. This was thermostatized with a peltier element, an LM35 temperature sensor, and custom feedback electronics. A magnetic stirrer provided solution homogeneity. Laser power was measured by directly hitting a light power meter and found to be constant throughout the experiments for all three lasers. Full spectra were acquired every 2 s with OOIChem software. Data fitting were carried out offline by numerical integration of the following expression:

$$dn_p/dt = I_{beam}(1 - 10^{-Abs_T})Abs_R/Abs_T\varphi$$

where n_p are the moles of released ligand, I_{beam} is the intensity of the incident light in Einsteins/s, Abs_T is the total absorbance of the solution at the beam's wavelength, Abs_R is the absorbance of **Ru-(dt3pya)$_2$** complex (see below) at the same wavelength, and Φ is the photolabilization quantum yield.

Factor analysis of the spectroelectrochemistry experiment was made as reported[26] using a two successive redox steps (C + 1 e^- → B, B + 1 e^- → A each one with a different value of E^0, with the analytical concentration of the initial sample) as fitting model.

Ditolyl-3-pyridylamine (dt3pya). One gram (5 mmol) of ditolylamine, 1.04 g (5 mmol) of 3-iodopyridine, 0.8 g (7 mmol) of potassium *tert*-butoxide, and 40 mg of a mixture of ratio 1:1 of CuI and 1−10 phenanthroline were dissolved in 10 mL of dry toluene. The mixture was heated over 12 h, refluxing at 110−115 °C, cooled, and then filtered to eliminate insoluble particles. The filtrate was adsorbed on silica Merck 60 and eluted using a solvent gradient (100% dichloromethane, dichloromethane ethyl acetate 98%/2%) in a 3 × 10 cm column. Yield: 0.9 g (65%). NMR ^{1}H (500 MHz, see Figure 1 for

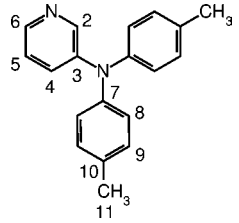

Figure 1. Ligand (ditolyl-3-pyridylamine, **dt3pya**) used in this study. Numeration relates to ^{1}H NMR characterization (see Experimental Section).

atom numbering): δ = 8.13 (H-2, bd, J = 3.8 Hz, 1H), 7.09 (H-4, m, 1H), 7.29 (H-5, ddd, J = 1.4, 2.9, 8.4 Hz, 1H), 8.32 (H-6, bs, 1H), 6.98 (H-8, d, J = 8.2 Hz, 4H), 7.08 (H-9, d, J = 8.2 Hz, 4H), 2.34 (H-11, s, 6H). NMR 13C: δ = 142.0, 144.7, 123.5, 128.3, 144.3, 124.7, 130.2, 133.5, 20.8.

[Ru(bpy)$_2$Cl-dt3pya] (PF_6) (Ru-dt3pya). A 100 mg portion of $[Ru(bpy)_2Cl_2]$ (0.2 mmol) was suspended in 5 mL of 96% ethanol and 2 mL of water under argon atmosphere. Then, 55 mg of **dt3pya** (0.2 mmol) and 200 mg of LiCl were added. The mixture was protected from light and heated to 90 °C until the spectrum remained unchanged. The solution was evaporated in darkness, redissolved in water and precipitated by adding drops of saturated NH_4PF_6 solution in water. The solid was filtered, redissolved in 3 mL of LiCl saturated acetone and refluxed over 1 h. This solution was dropped into water (with continuous stirring), rendering a red precipitate which was filtered and washed several times with cold water. This procedure for separation and storage had to be carried out in darkness because of the photolability of **dt3pya**. Yield: 120 mg (70%). 1H NMR (500 MHz, acetone-d6): δ = 2.33 (s, 6H), 6.78 (d, J = 7.6 Hz, 4H), 7.00 (d, J = 7.7 Hz, 2H), 7.04 (d, J = 7.6 Hz, 4H), 7.05 (d, J = 8.4 Hz, 1H), 7.11 (d, J = 7.8 Hz, 1H), 7.22 (d, J = 8.7 Hz, 1H), 7.27 (s, 1H), 7.46 (d, J = 5.6 Hz, 1H), 7.51 (d, J = 4.2 Hz, 1H), 7.58 (m, 2H), 7.63 (q, J = 8.4, 8.4, 8.4 Hz, 2H), 8.06 (t, J = 7.8, 7.8 Hz, 1H), 8.00 (t, J = 7.8, 7.8 Hz, 1H), 8.11 (d, J = 8.0 Hz, 1H), 8.16 (d, J = 8.1 Hz, 1H), 8.33 (dd, J = 7.9, 2.4 Hz, 2H), 8.59 (d, J = 5.4 Hz, 1H), 9.85 (d, J = 4.9 Hz, 1H). ESI-MS: m/z calcd for $C_{39}H_{34}ClN_6Ru$ ($[Ru(bpy)_2ClL]^{1+}$): 723.1577; found: 723.1578.

[Ru(bpy)$_2$(dt3pya)$_2$](PF_6)$_2$ (Ru-(dt3pya)$_2$). A 100 mg portion of $[Ru(bpy)_2Cl_2]$ (0.2 mmol) was suspended in 6 mL of water and heated to 90 °C under argon atmosphere. Labilization of Cl^- to form $[Ru^{II}(bpy)_2(H_2O)_2]^{2+}$ (λ_{max} = 480 nm) was completed after 1 h. Then, 110 mg (0.4 mmol) of **dt3pya** dissolved in 1.5 mL of 96% ethanol was added. The resulting suspension was heated with stirring at 90 °C for 12 h in darkness, and kept in an argon atmosphere until full displacement of water by **dt3pya**. The orange solution was filtered to

dx.doi.org/10.1021/ic200966f | Inorg. Chem. 2012, 51, 1261−1268

Table 1. MLCT Maxima, Redox Potential and Photolabilization Quantum Yield for *cis*-$[Ru^{II}(bpy)_2XY]$ Complexes

X−Y ligand	λ MLCT (nm)	$Ru^{III/II}$ (V)[a]	$L_1^{+/0}$ (V)[a]	$L_2^{+/0}$ (V)[a]	Φ[b]
Cl_2	553, 380[c]	0.53[c]			
Cl− L	502[d]	1.07[d]	1.46[d]		
L_2	461[d]	1.39[d] (1.37[e])	1.39[d] (1.41[e])	1.80[d]	0.11[d]
$(3ampy)_2$[f]	463[g]	1.42[g]			0.08[d]

[a]In acetonitrile. [b]In acetone. [c]Ref 26. [d]This paper. [e]From factor analysis. [f]3-ampy is 3 aminopyridine. [g]Ref 24.

remove insoluble materials, and the filtrate was precipitated by adding drops of saturated NH_4PF_6 solution. The suspension was filtered (or centrifuged) and washed several times with cold water. The procedure for separation and storage had to be carried out in the dark because of the photolability of **dt3pya**. Yield: 200 mg (80%). ^{1}H NMR (500 MHz, acetone-d6) δ = 2,34 (s, 12H), 6.94 (m, 8H), 7.21 (m, 10H), 7.31 (m, 2H), 7.38 (dd, J = 8.6, 2.5 Hz, 2H), 7.68 (d, J = 2.5 Hz, 2H), 7.78 (d, J = 5.0, 2H), 7.98 (d, J = 5.0, 2H), 7.98 (td, J = 6.8, 1.4 Hz, 2H), 8.05 (td, J = 8.0, 1.4 Hz, 2H), 8.34 (td, J = 8.0, 1.4 Hz, 2H), 8.58 (d, J = 8.0 Hz, 2H), 8.69 (d, J = 8.0 Hz, 2H), 8.89 (d, J = 5.0 Hz, 2H). ESI-MS: m/z calcd for $C_{58}H_{52}N_8Ru$ ($[Ru(bpy)_2L_2]^{2+}$): 481.1679; found: 481.1666.

RESULTS AND DISCUSSION

Figure 1 shows the ligand **dt3pya** (ditolyl-3-pyridylamine) used in this study. The ^{1}H NMR spectrum of **Ru-dt3pya** showed a complex set of signals (34 protons in 19 signals), reflecting the asymmetry of substitution at the *cis* positions (Cl^- and **dt3pya**). In contrast, the spectrum of **Ru-(dt3pya)$_2$** showed 52 protons in only 14 signals, corresponding to a more symmetrical compound. This is consistent with the rotation of coordinated **dt3pya** which, for NMR spectroscopy time scales, dynamically averages the field seen by other protons and presents both *cis* substitution sites as indistinguishable. A similar effect was already observed in mono and disubstituted analogues with 4-aminopyridine.[27] A preliminary observation of possible coordinated **dt3pya** movements in **Ru-(dt3pya)$_2$**[28] shows that the rotation of the ligand is possible, but needs to be concerted with the other ligand to generate enough space to allow full movement (especially regarding the independent rotation of the pyridine).[29]

Table 1 shows a comparison of basic information between $[Ru(bpy)_2Cl_2]$, **Ru-dt3pya**, and **Ru-(dt3pya)$_2$** in terms of MLCT (acetonitrile), photolabilization quantum yield (acetone), and redox potential (acetonitrile), together with $[Ru(bpy)_2(3\text{-aminopyridine})_2]^{2+}$. Electronic spectroscopy showed that MLCT $Ru^{II} \rightarrow$ bpy* charge transfer shifted to higher energies as Cl^- was replaced by **dt3pya** (553, 502, and 461 nm for Cl_2, Cl-**dt3pya**, and **dt3pya$_2$**, respectively). This is a common motif for acceptor ligands because of the stabilization of Ru^{II} t_{2g} orbitals after mixing with π^* of the ligand,[30] and it is also reflected in a redox potential shift to oxidant values (0.53, 1.07, 1.41 V for the same complexes). Comparsion of **Ru-(dt3pya)$_2$** with $[Ru(bpy)_2(3\text{-aminopyridine})_2]^{2+}$ reveals a very similar MLCT (461 nm vs 463 nm), E^0 (1.41 V vs 1.42 V, see bellow), and photolabilization quantum yield (0.11 vs 0.08, see bellow) that suggests conjugation with phenyls has little effect on the π donor and π acceptor capabilities of **dt3pya** compared with unsubstituted 3-aminopyridine.

The chemistry of $[Ru^{II}(bpy)_2L_2]^{2+}$ (L = aliphatic or aromatic amine) is characterized by the photolabilization of ligand L,[31] which is responsible for the need to avoid light during the synthesis of these compounds. This property has made them promising as scheduled-delivery neurotransmitter agents in living tissues, with verified physiological activity only when illuminated.[27] Consistently with this behavior, the NMR spectrum of irradiated solutions of **Ru-(dt3pya)$_2$** showed the appearance of the methyl signals of the free ligand **dt3pya** at 2.31 ppm, as well as a decrease in the integration of the coordinated ligand at 2.34 ppm (Supporting Information S1). Changes in the UV−vis spectrum of the solution during irradiation are shown in Figure 2, from which we fit a value of ϕ = 0.11 (quantum yield) for **dt3pya** release in **Ru-(dt3pya)$_2$**.

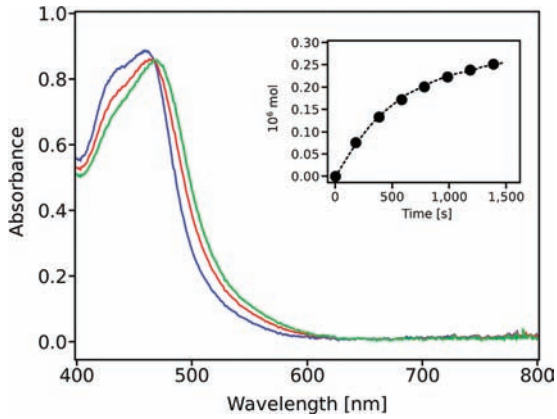

Figure 2. UV−vis spectra of **Ru-(dt3pya)$_2$** in acetone during irradiation at 473 nm. Inset: moles of released ligand vs time.

The quantum efficiencies for labilization depend on the stationary population of the e_g dissociative state during the de-excitation pathway following irradiation. This state increases its participation in the decay mechanism as the π acceptor ability of ligands moves the MLCT state (and the triplet emitter state) above e_g.[31] In practice, this means that π acceptor ligands (which blue-shift the energy of the MLCT $Ru^{II} \rightarrow$ bpy*) propitiate photolabilization. By contrast, π donor ligands (CN^-, SCN^-, for example) increase the e_g state energy above the triplet emitter state, which makes these complexes substitutionally photoinert, suitable for practical uses in charge transfer devices. An example of this is the reported electron injection into TiO_2 from the bpy centered excited state of the $[Ru^{II}(bpy)(SCN)_2]^0$ fragment.[20] In this system, the ruthenium center is bound to an arylamine-like ligand that plays the role of a temporary sacrificial electron-donating reagent. The technological uses of this kind of compounds involve achieving a device with components in a spatial organization (usually layers in a high surface electrode) so that the movement of electrons generated from light absorption has a defined direction and sense.

The cyclic (CV) and square wave (SWV) voltammograms of **Ru-dt3pya** in Figures 3a−b show two peaks associated to bpy coligands reduction at −1.19 V and −1.42 V. At oxidizing potentials **Ru-dt3pya** showed two independent one-electron redox waves at 1.07 and 1.46 V (same current as reduction waves). Since the spectroelectrochemistry of **Ru-dt3pya** at

dx.doi.org/10.1021/ic200966f | Inorg. Chem. 2012, 51, 1261−1268

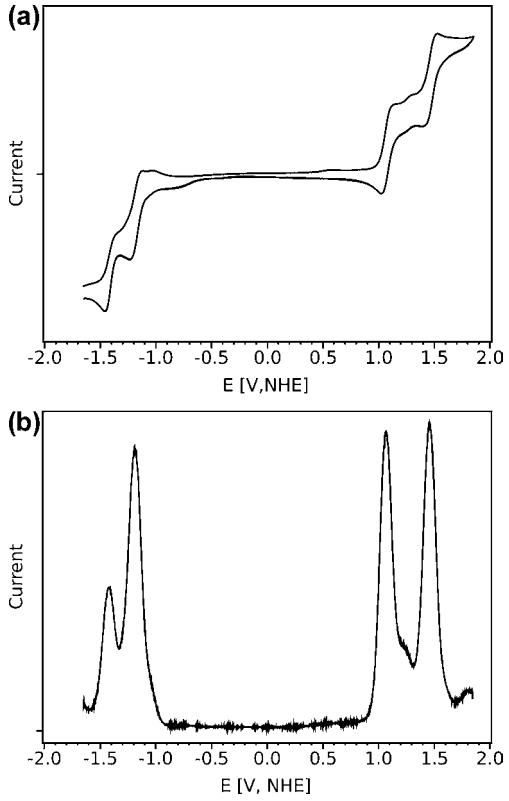

Figure 3. Voltammograms of **Ru-dt3pya** in acetonitrile 0.1 M $TBAPF_6$: (a) CV (100 mV/s), (b) SWV (25 Hz, 2 mV/step).

Figure 4 showed that a decay of the MLCT $Ru^{II} \rightarrow$ bpy is associated with the first wave at 1.07 V, we assigned this process

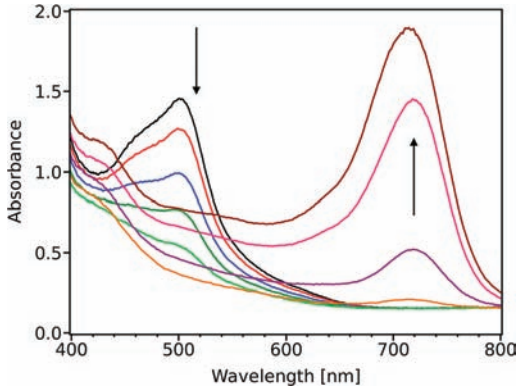

Figure 4. Spectroelectrochemistry of **Ru-dt3pya** in acetonitrile, 0.1 M $TBAPF_6$, from 0.9 to 1.7 V.

to a Ru^{II} oxidation. The later appearance of a band at 720 nm, similar to that of radicals derived from tritolylamine,[32] suggests (consistently) that the second redox process at 1.46 V corresponds to the oxidation of a redox-active ligand **dt3pya**.

The voltammograms of **Ru-(dt3pya)$_2$** in Figure 5a–b showed two bpy reductions at −1.06 V and −1.25 V. The higher reduction potential compared to **Ru-dt3pya** reflects the effect that metal electron density is shared with a more extended π system (two **dt3pya** for backbonding, instead of one) and then bpy coligands are slightly less electron rich. A similar shift has been observed for a series of reported complexes,[33] although with lower sensitivity.[34] Second, two waves were found at oxidant potentials. One appears at 1.39 V, and it shows in the CV a current peak twice the intensity than each bpy monoelectronic reduction. Since the diffusion coefficient for the initial specie in the voltammogram is the same for both current waves (reduction and oxidation), we infer that the wave at 1.39 V involves two electrons. The second wave in **Ru-(dt3pya)$_2$** appears at 1.80 V and was not reversible.[35]

Since we have three redox centers in this complex and the wave at 1.39 V seems to be a bielectronic one, we need to assign which of the redox centers were first oxidized to understand the intervalence properties that we will see below. Only two scenarios are expected for the dioxidized specie: in scenario "a" one ligand and the metal are oxidized, in scenario "b" both ligands are oxidized.

Supporting scenario "a", from Table 1 we see that **dt3pya** oxidation in **Ru-dt3pya** appears at 1.46 V and Ru oxidation in $[Ru(bpy)_2(3ampy)_2]^{2+}$ appears at 1.42 V, both values very close to the two electron wave at 1.39 V. This comparison suggests that one ligand and the ruthenium center would be the first oxidized fragments.

On the other hand, it is established that the contributions of the ligands to the redox potential of $Ru^{III/II}$ center can be factored into σ and π interactions with the metal, and are approximately additive.[36] This is verified, for example, in successive replacements of Cl^- by pyridine[31] in the following series: $[Ru(bpy)_2Cl_2]$ (0.53 V), $[Ru(bpy)_2ClPy]^+$ (1.02 V), and $[Ru(bpy)_2(Py)_2]^{2+}$ (1.53 V). Since the redox potential shift between $[Ru(bpy)_2Cl_2]^0$ and **Ru-dt3pya** was ≈0.5 V, we estimate that the resulting shift when replacing both Cl^- ligands by two **dt3pya** should locate the redox couple $Ru^{III/II}$ at about 1.61 V, which falls halfway between the first oxidation wave at 1.39 V and the second one at 1.80 V. This estimation is consistent with the simultaneous oxidation of both **dt3pya** (scenario "b") at 1.39 V and the Ru oxidation at a potential higher than 1.61 V (1.80 V), because it would be coordinated to two positive (then, more acceptor after oxidation) ligands. Next, we look at the spectroscopic information.

Figure 6a–b shows four spectra of the spectroelectrochemistry experiment of **Ru-(dt3pya)$_2$** inside the 1.39 V redox wave and the absorbance changes at 712 y 1425 nm. It is clear that the first spectral change in this wave (spectrum b) is the appearance of a band at 712 nm without any absorption in the NIR.[37] This band is characteristic of triarylamine radicals, similar to the one found at 720 nm in the second oxidation of **Ru-dt3pya**, and supports that the first process at the bielectronic wave is the oxidation of the coordinated ligand, yielding **Ru^{II}-dt3pya$^+$-dt3pya**. This assignment is consistent with both scenarios depicted above.

Following the spectroelectrochemistry experiment at 1.39 V, the absorbance profiles in Figure 6b show that the second oxidation occurs a few millivolts after the first one, and that it is clearly associated with the NIR band at 1425 nm. After full development of this band, the spectrum starts changing in a way that depends not only on potential but mainly of time. We associate this process to the irreversibility of the wave at 1.80 V, and it will be discussed below.

Factor analysis with NIPALS algorithm[26] was used to process data from the spectroelectrochemistry experiment, fitting the spectra and concentrations profiles obtained by the method to the simplest model of two successive redox steps (see Experimental Section). Values of 1.37 and 1.41 V for each redox process were found, and the three spectra of pure

dx.doi.org/10.1021/ic200966f | Inorg. Chem. 2012, 51, 1261–1268

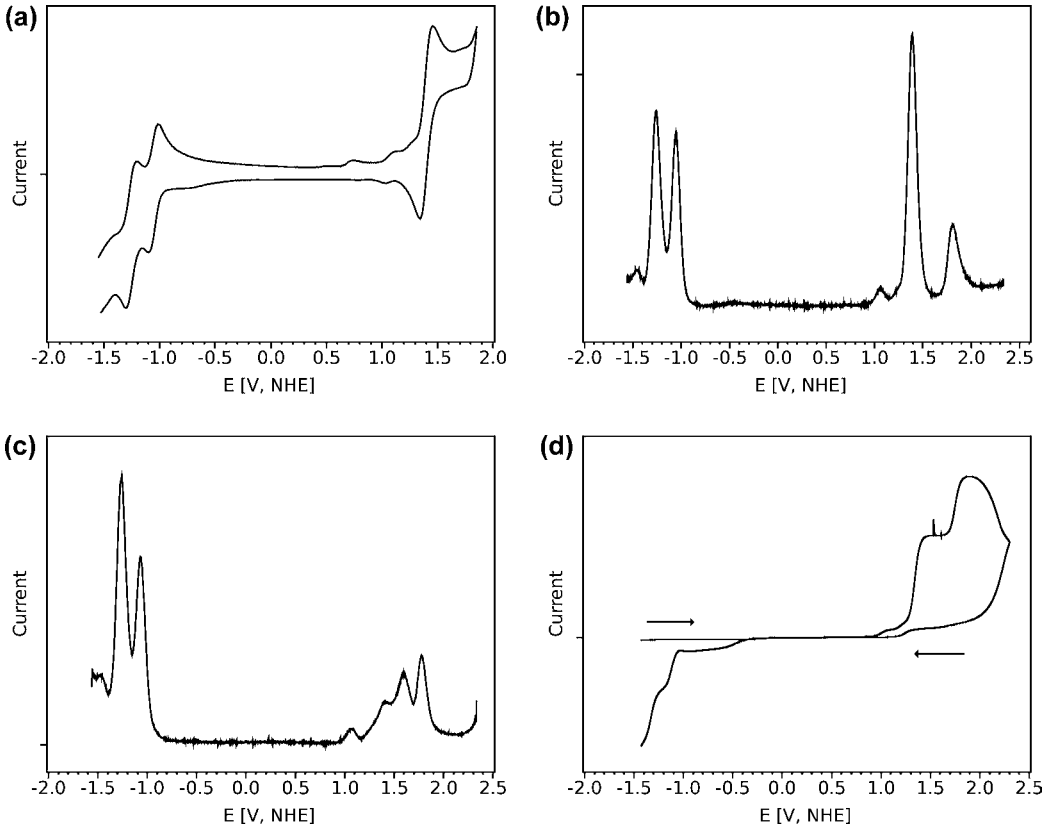

Figure 5. Voltammograms of **Ru-(dt3pya)$_2$** in acetonitrile 0.1 M TBAPF$_6$: (a) CV (500 mV/s), (b) SWV (25 Hz, 2 mV/step), (c) SWV (25 Hz, 2 mV/step) starting a 2 V downward, and (d) CV (20 mV/s).

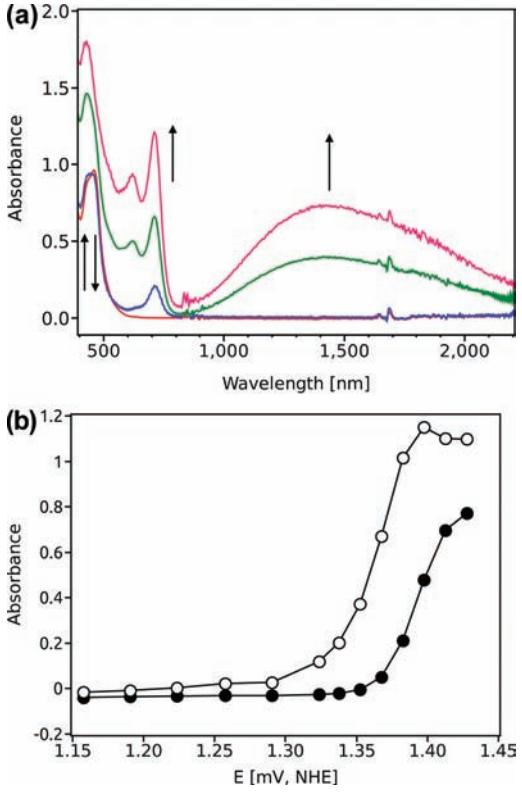

Figure 6. Spectroelectrochemistry of **Ru-(dt3pya)$_2$**, 0.1 M TBAPF$_6$: (a) from 1.15 to 1.45 V, (b) Absorbance profiles at 712 nm (white circles) and 1425 nm (black circles).

calculated species are shown in Figure 7a–b, along with fitted concentration profiles. The first specie is assigned to the **Ru-(dt3pya)$_2$** initial complex, with absorption at 461 nm (MLCT Ru^{II} → bpy*). The second specie shows absorption at 712 nm and a band at 450 nm. The third specie shows a broad absorption at 1425 nm and a small band at 620 nm. The absorption at 450 nm is displaced to 430 nm and resembles the shape of $[Ru^{III}(bpy)_3]^{3+}$ system, although not conclusively.

Consistently with both scenarios regarding the assignment of the dioxidized specie, it is clear that the first process in the two overlapped electron waves at 1.39 V (1.37 V from the factor analysis fitting) yields **Ru^{II}-dt3pya$^+$-dt3pya** because we found a radical absorption at 712 nm that precedes any other spectral change. This system does not show a strong NIR intervalence band, so we infer that the Ru^{II} center is not a good coupling bridge to electronically communicate an intervalence system formed by two coordinated redox-active donor ligands, one of them being oxidized. It is remarkable that the innocuous electronic role played by Ru^{II} in the **dt3pya$^+$-dt3pya** coordinated intervalence system contrasts with the redox splitting effect observed with the metal in the same oxidation state (2+) but now in the **bpy$^-$-bpy** system, with a ΔE^0 = 0.2 V (see bpy reductions in Figures 3b and 5b).

Once the first process is clarified, it is in the second electron process where scenarios "a" and "b" actually differ. One possibility is that the second ligand gets oxidized while keeping ruthenium at 2+ state (scenario "a"). In such a case, then, oxidation of both **dt3pya** would be separated by only 40 mV because of the Ru^{II} effect. Arylamines mixed valence compounds have shown empirically smaller separations of redox potential compared to classical metal mixed-valence

dx.doi.org/10.1021/ic200966f | Inorg. Chem. 2012, 51, 1261–1268

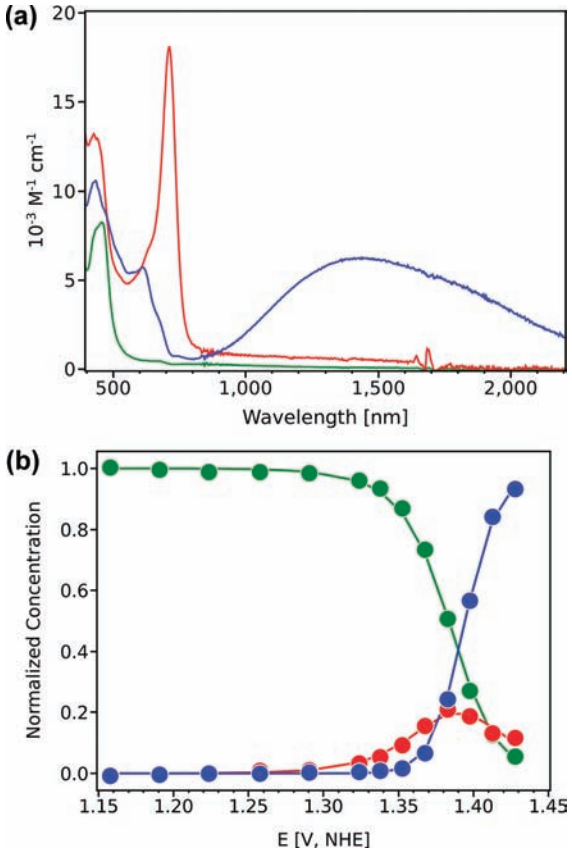

Figure 7. Information from factor analysis using Nipals algoritm (see text): (a) Spectra of $\mathbf{Ru^{II}}$-**(dt3pya)**$_2$ (green), $\mathbf{Ru^{II}}$-**dt3pya**$^+$-**dt3pya** (red, absorbance reduced by a factor of 2) and $\mathbf{Ru^{III}}$-**dt3pya**$^+$-**dt3pya** (blue), (b) Relative concentration profiles vs potential for the same species (same colors).

compounds[38,39] but, even for small separations, a noticeable absorption in the NIR is always observed for the single oxidized mixed valence system. Moreover, no intervalence band would be observed for the doubly oxidized system. Any of those observations are verified in the spectra of Figure 6a, so we conclude that scenario "a" is not possible.

The other possibility (scenario "b") is that ruthenium oxidizes at 1.41 V to 3+ state, so the dioxidized specie would be $\mathbf{Ru^{III}}$-**dt3pya**$^+$-**dt3pya**. This would make the spectrum with bands at 1425 and 620 nm the intervalence electronic spectroscopy of a system of two aryalmines bridged by Ru^{3+}. The most closely related spectroscopic example to our proposal of ligand-to-ligand charge transfer between arylamines is a set of organic compounds consisting of substituted tetraphenylbenzidines (TPB, a triarylamine dimer) containing methyl groups at the central benzidine rings.[40] The steric hindrance of the central methyl groups twists the molecule and leads to a progressive loss of planarity in the conjugated π system. This structural feature is associated with the coexistence of both the intervalence transition at the NIR (at 1876 nm for the intermediate-coupled benzidines and 1467 nm for the full coupled system) and a displacement of the arylamine radical absorption (from ca. 750 nm in free tritolylamine to 685 nm in the intermediate-coupled benzidine, and 484 nm in the full coupled one). The effect is rationalized by assuming a variable π orbital overlap between arylamine fragments, depending on the angle between phenyl planes. The spectrum of dioxidized **Ru-(dt3pya)**$_2$, with bands at 1435 and 620 nm, locates the electronic structure of this complex between the intermediate-coupled benzidines and the full coupled ones (compounds 5a and 4 in ref 40). For this reason, we assign the dioxidized specie to $\mathbf{Ru^{III}}$-**dt3pya**$^+$-**dt3pya** (scenario "b") and, according to the spectrum, we infer that the Ru^{3+} effectively couples both arylamines. This system mediated by Ru^{3+} contrasts with the isolated arylamine system bridged by Ru^{2+}.[41]

The second oxidation wave in **Ru-(dt3pya)**$_2$ (third electron from the starting compound) appeared at 1.80 V in SWV and showed to be irreversible in the CV experiment at low speed (50 mV/s in the 50 μm electrode). It also made the first wave at 1.39 V irreversible, which showed a reversible electrochemistry provided the potential did not exceed 1.80 V. This irreversibility is clearly seen in the SWV reversing scan (from 2.00 V downward, Figure 5c) because, at decreased speeds, a new chemical specie with its own redox activity appeared at 1.59 V. At faster scan rates (1 V/s), both the SWV and CV showed quasi-reversible voltammograms, although not fully reversible. At very slow sweeps (10 mV/s), as the potential in the CV increased beyond 1.80 V, the overall current decreased and the voltammogram returned to cathodic potentials with no current (Figure 5d). The electrode surface could be regenerated from this passivation by a fast cycling (5 cycles) between −2.00 and 2.00 V. This effect was related to the time spent at oxidizing potentials rather than to the potential itself, as long as it remained over 1.80 V.

The fact that the electrochemical irreversibility was manifested only when the two ligands **dt3pya** were simultaneously oxidized suggests that a coupled chemical process, similar to the dimerization of triphenylamine (TPA), occurs inside the coordination sphere.[42] In the oxidized radical TPA, a Lewis base (acetonitrile, for example) removes protons in positions 4 to the arylamine nitrogen, letting the unpaired electrons expose to the solution. A bimolecular process involving two identical radicals results in the formation of a carbon-to-carbon covalent bond to yield a tetraphenylbenzidine derivative. In our system, this would give the ligand 5,5′-bis(ditolylamino)-2,2′-bipyridine (Scheme 1).

Scheme 1. Oxidation Scheme of Coordinated Ligands beyond 1.80 V

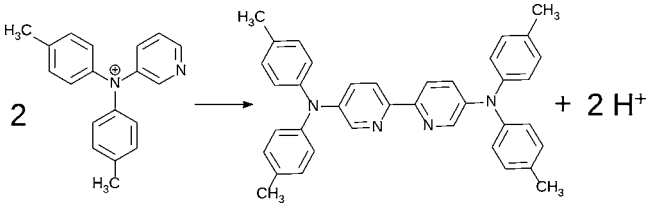

Using the MLCT $Ru^{II} \rightarrow$ bpy* in **Ru-dt3pya** as absorptivity calibration (ε = 7750 M^{-1} cm^{-1}), we estimated 6050 M^{-1} cm^{-1} for molar absorptivity of the intervalence band (both in acetonitrile). This band gives an oscillator strength of f = 0.12 and a transition moment of 1.25 eÅ. Assuming an average diabatic separation distance of 7.5 Å,[43] we estimated a dipole moment change upon absorption of 7.1 eÅ (95% of the diabatic distance), a mixture of 3% between diabatic states, and an effective ligand coupling of 1200 cm^{-1}, all these figures being under an effective two-state electronic model.[5,44]

Lambert and Launay have analyzed intervalence systems containing arylamines based on a quantitative model of three electronic interacting diabatic states,[45,46] with individual

dx.doi.org/10.1021/ic200966f | Inorg. Chem. 2012, 51, 1261−1268

coupled oscillators representing the influence of the reaction coordinate on the energies of the associated electronic states (see especially Figure 4b of ref 45). Applying a three-state analysis to our system involves considering (a) the dioxidized and diabatic states **Ru^{II}-dt3pya^{+}-dt3pya^{+}**, **Ru^{III}-dt3pya^{+}-dt3pya**, and **Ru^{III}-dt3pya-dt3pya^{+}**; (b) an electronic coupling only between chemical bond adjacent sites; and (c) reorganization energies λ_m (for the fragment $[Ru(bpy)_2]$) and λ_l (for each of the two ligands **dt3pya**). While it is not possible to obtain all necessary data to analyze our system quantitatively, we can make several valuable observations at a qualitative level using this approach.

The single-oxidized species **Ru-dt3pya** generated in the spectroelectrochemistry experiment only shows absorbance toward the UV (above 400 nm) where intraligand bpy $\pi \rightarrow \pi^*$ bands appear. Since we were unable to locate the LMCT **dt3pya** $\rightarrow$ Ru^{III} in the visible-NIR region, we estimated this metal–ligand coupling element from measurements on related compounds. A large number of charge transfer parameters in the series $[Ru^{II/III}(NH_3)_5L]^{2+/3+}$ by electroabsorption (Stark) spectroscopy have been reported.[44] From the LMCT transition in $[Ru^{III}(NH_3)_5$-4-aminopyridine$]^{3+}$ at 511 nm, it follows a metal–ligand coupling of 3400 cm^{-1} (0.42 eV), similar to other Ru^{III} with pyridinic ligands. This coupling value is an excess estimation for the chromophore Ru^{III}-**dt3pya** because Ru^{III} orbitals are partially involved in π interactions with bpy coligands and are less available to overlap with the π system of **dt3pya**. As the ligand, the delocalization of **dt3pya** because of phenyl groups compared to 4-aminopyridine also limits the π orbital overlapping with the metal. For these two reasons, we assume that the metal–ligand coupling (in **Ru-dt3pya** as in **Ru-(dt3pya)$_2$**) will be lower than in the $[Ru^{III}(NH_3)_5$-4-aminopyridine$]^{3+}$.

It has been estimated that the internal reorganization energy of tritolylamine (a reasonable approximation of **dt3pya**) at DFT-B3LYP-6-31G* level is 0.14 eV.[47] This value is about half the internal reorganization energy in octahedral $d^{6/5}$ low spin coordination compounds of similar size, which is roughly estimated at 0.24 eV.[5] Considering that the external reorganization adds about 0.7 eV for a charge-separated specie like **Ru-(dt3pya)$_2$** in a polar solvent like acetonitrile,[5] both λ_l and λ_m result larger than the estimated coupling. This places the **Ru-(dt3pya)$_2$** system at Class 2 (according to Robin and Day's classification) but coupled enough to stay in the adiabatic regime.[5] This is consistent with the properties of the intervalence transition analyzed above (3% delocalization).

The fact that the spectrum of dioxidized **Ru-(dt3pya)$_2$** greatly resembles that of partially twisted benzidines suggests that the unpaired electron circulates primarily by a minimum energy at the potential surface associated with **Ru^{III}-dt3pya^{+}-dt3pya** and **Ru^{III}-dt3pya-dt3pya^{+}** states or, in Lambert's nomenclature,[45] the triarylamine radical cation state centers. Moreover, the minimum on that surface energy associated with the remaining state **Ru^{II}-dt3pya^{+}-dt3pya^{+}** (the bridge state in terms of Lambert's model) is either not accessible at the experiment temperature or, at least, the concentration is not spectroscopically detectable. This is only possible if the diabatic state **Ru^{II}-dt3pya^{+}-dt3pya^{+}** is at a higher energy than the other two states involving Ru^{III}. Therefore, the surface for **Ru-(dt3pya)$_2$** is similar to the one depicted by Lambert in Figure 4 of ref 45.

Whereas delocalized benzidine[40] reaches about 300 mV in ΔE and localized twisted benzidine about 150 mV, almost 400 mV separation between the first and second **dt3pya** in **Ru-(dt3pya)$_2$** (from 1.37 to 1.80 V) suggests an odd communication effect of d^5 Ru^{III} that does not match the information of electronic spectroscopy (a coupled although localized system). Unlike linear (usually trans) intervalence compounds, **dt3pya** in **Ru-(dt3pya)$_2$** are in adjacent positions, with solvent in between. Analytical solvation models used in electron transfer do not consider dielectric polarization inside the intervalence cavity, where it is expected that the electric field has a much stronger effect aligning the solvent dipoles compared to the electric field outside the system. Since these models assume linear species, we are not currently able to estimate quantitatively the electrostatic and solvation influence in ΔE to asses whether this splitting in redox potential is reasonable or not.

CONCLUSIONS

We here found qualitative evidence of the different capabilities of the bridges $[Ru^{II}(bpy)_2]^{2+}$ and $[Ru^{III}(bpy)_2]^{3+}$ to electronically connect an intervalence system consisting of two arylamine-like redox-active ligands. The mixed valence behavior of this ligand–metal–ligand system seems to follow the same rules as the classical metal–ligand–metal system, since the best bridges for coupling sites are those with complementary π orbital interactions, for example, the combination of either π^* empty acceptor bridges like pyrazine and donor d^6 metals such as $[Ru^{II}(NH_3)_5]^{2+}$ or π donors bridges like dicyanobenzene with the oxidized acceptor fragment $[Ru^{III}(NH_3)_5]^{3+}$.[6] Applied into our system **Ru-(dt3pya)$_2$**, the π donor properties of neutral arylamines (popular hole transport material for this reason) are matched to the d^5 acceptor ability of $[Ru^{III}(bpy)_2]^{3+}$ to give a Class II compound **dt3pya-dt3pya^{+}** by the superexchange mechanism. In contrast, the donor fragment $[Ru^{II}(bpy)_2]^{2+}$ is not able to interact either with neutral or with oxidized arylamine, giving a Class I intervalence system. However, the same Ru^{II} fragment is able to interact with π^* empty acceptor orbitals in bpy and, when one of the ligands is reduced, they become a Class II intervalence system where Ru^{II} is an efficient communicating bridge.

Future efforts will focus on obtaining derivatives with CN^-, SCN^-, and carboxypyridine to prevent photolabilization and allow studying the photophysics of the ruthenium-arylamine interaction in the context of solar cells. Ligand derivatization will allow changing arylamines and ruthenium redox potentials to continue exploring the role of the metal oxidation state in the ligand–ligand mixed valence properties. We will also explore the reactivity of coordinated diphenyl-3-aminopyridine (the use of phenyl instead of tolyl would form polymers), and diphenyl-4-aminopyridine (which should not participate in irreversible reactions after oxidation). Theoretical studies will also help in a deeper and quantitative understanding of the electronic structure and intervalence properties of these compounds.

ASSOCIATED CONTENT

Supporting Information

A graph containing NMR signals at methyl resonance region before and after irradiation a 473 nm, with integrations. This material is available free of charge via the Internet at http://pubs.acs.org.

dx.doi.org/10.1021/ic200966f | Inorg. Chem. 2012, 51, 1261–1268

AUTHOR INFORMATION

Corresponding Author

*E-mail: aparise@mdp.edu.ar.

ACKNOWLEDGMENTS

This research was supported by the National Agency for Science and Technology Promotion (ANPCYT, PICT 213). A.R.P. and R.E. are members of CONICET. C.L.R. and O.F. thank CONICET for graduate fellowships. We thank Néstor Katz for reading the manuscript and valuable discussions.

REFERENCES

(1) Robin, M. B.; Day, P. *Adv. Inorg. Chem. Radiochem.* **1967**, *10*, 247−422.

(2) Allen, G. C. *Hush, N. S. Prog. Inorg. Chem.* **1967**, *8*, 357−389.

(3) Hush, N. S. *Prog. Inorg. Chem.* **1967**, *8*, 391−444.

(4) Day, P. *Int. Rev. Phys. Chem.* **1981**, *1*, 149−193.

(5) Creutz, C. *Prog. Inorg. Chem.* **1983**, *30*, 1−73.

(6) Crutchley, R. J. *Adv. Inorg. Chem.* **1994**, *41*, 273−325.

(7) Brown, D. B., Ed.; *Mixed-Valence Compounds: Theory and Applications in Chemistry, Physics, Geology, and Biology*; Reidel Publishing Company: Dordrecht, The Netherlands, 1980; NATO ASI Series D.

(8) Prassides, K., Ed.; *Mixed Valence Systems: Applications in Chemistry, Physics and Biology*; Kluwer Academic Publishers: Dordrecht, The Netherlands, 1991; NATO ASI Series C, Vol *343*.

(9) (a) Demadis, K. D.; Hartshorn, C. M.; Meyer, T. J. *Chem. Rev.* **2001**, *101*, 2655−2686. (b) Brunschwig, B. S.; Creutz, C.; Sutin, N. *Chem. Soc. Rev.* **2002**, *31*, 168−184.

(10) Day, P.; Hush, N. S.; Clark, R. J. H. *Philos. Trans. R. Soc., A* **2008**, *366*, 5−14 , and references in the same issue.

(11) Soncini, A.; Mallah, T.; Chibotaru, L. F. *J. Am. Chem. Soc.* **2010**, *132*, 8106−8114.

(12) Nocera, D. G. *Inorg. Chem.* **2009**, *48*, 10001−10017.

(13) (a) Lu, Y.; Quardokus, R.; Lent, C. S.; Justaud, F.; Lapinte, C.; Kandel, S. A. *J. Am. Chem. Soc.* **2010**, *132*, 13519−13524. (b) Lent, C. S.; Isaksen, B.; Lieberman, M. *J. Am. Chem. Soc.* **2003**, *125*, 1056−1063.

(14) Nelsen, S. F.; Ismagilov, R. F.; Trieber, D. A. *Science* **1997**, *278*, 846.

(15) Acosta, A.; Zink, L. I.; Cheon, J. *Inorg. Chem.* **2000**, *39*, 427−432.

(16) Metcalfe, R. A.; Lever, A. B. P. *Inorg. Chem.* **1997**, *36*, 4762−4771.

(17) (a) Balzani, V.; Bergamini, G.; Marchioni, F.; Ceroni, P. *Coord. Chem. Rev.* **2006**, *250*, 1254−1266. (b) Kalyanasundaram, K. *Coord. Chem. Rev.* **1982**, *46*, 159−244. (c) Juris, A.; Balzani, V.; Barigelletti, F.; Campagna, S.; Belser, P.; von Zelewsky, A. *Coord. Chem. Rev.* **1988**, *84*, 85−277.

(18) Concepcion, J. J.; Jurss, J. W.; Brennaman, M. K.; Hoertz, P. G.; Patrocinio, A. O. T.; Iha, N. I. M.; Templeton, J. L.; Meyer, T. J.. *Acc. Chem. Res.* **2009**, *42*, 1954−1965.

(19) Grätzel, M. *Acc. Chem. Res.* **2009**, *42*, 1788−1798.

(20) Jin, Z.; Masuda, H.; Yamanaka, N.; Minami, M.; Nakamura, T.; Nishikitani, Y. *Phys. Chem. C* **2009**, *113*, 2618−2623.

(21) Jiang, Z.; Ye, T.; Yang, C.; Yang, D.; Zhu, M.; Zhong, C.; Qin, J.; Ma, D. *Chem. Mater.* **2011**, *23*, 771−777.

(22) Perrin, D. D.; Armarego, W. L. F. *Purification of Laboratory Chemicals*, 3rd ed.; Pergamon Press: Oxford, U.K., 1988.

(23) (a) Sullivan, B. P.; Salmon, D. J.; Meyer, T. J. *Inorg. Chem.* **1978**, *17*, 3334. (b) Viala, C.; Coudret, C. *Inorg. Chim. Acta* **2006**, *359*, 984−989.

(24) Ellis, C. D.; Margerum, L. D.; Murray, R. W.; Meyer, T. J. *Inorg. Chem.* **1983**, *22*, 1283−1291.

(25) Noviandri, I.; Brown, K.; Leming, D. S. *J. Phys. Chem. B* **1999**, *103*, 6713−6722.

(26) (a) Scarminio, I.; Kubista, M. *Anal. Chem.* **1993**, *65*, 409−416. (b) Kubista, M.; Sjoeback, R.; Albinsson, B. *Anal. Chem.* **1993**, *65*, 994−998.

(27) Zayat, L.; Calero, C.; Alborés, P.; Baraldo, L.; Etchenique, R. *J. Am. Chem. Soc.* **2003**, *125*, 882−883.

(28) Ru-N(pyridine) bond rotation with fixed inter atomic distances calculated by DFT-B3LYP-LANL2DZ.

(29) All attempts to obtain single crystals to clarify this issue were so far unsuccessful. However, crystal packaging could not represent the dynamic behavior of the ligands in solution, and electrostatic interactions could make some specific configuration preferable.

(30) Not to be confused with the π^* of bpy coligands, which remains at about the same energy in different complexes. Indeed, the $bpy^{-/0}$ redox potential does not change significantly in a series of Ru^{II} complexes. The reason why MLCT $Ru^{II} \rightarrow$ bpy* shifts is mainly the stabilization of t_{2g} orbitals.

(31) Pinnick, D. V.; Durham, B. *Inorg. Chem.* **1984**, *23*, 1440−1445.

(32) Sreenath, K.; Suneesh, C. V.; Gopidas, K. R.; Flowers, R. A. II *J. Phys. Chem. A* **2009**, *113*, 6477−6483.

(33) Caspar, J.; Meyer, T. J. *Inorg. Chem.* **1983**, *22*, 2444−2453.

(34) For the same set of ligands, $bpy^{+/0}$ redox potential spans along 0.2 V while $Ru^{III/II}$ spans 0.8V. See ref 33.

(35) Note that the voltammogram in Figure 5a does not reach the wave at 1.80 V, while the pulsed experiment in Figure 5b does. This wave makes the process at 1.39 V become irreversible. See Figures 5c−d.

(36) (a) Fielder, S. S.; Osborne, M. C.; Lever, A. B. P.; Pietro, W. J. *J. Am. Chem. Soc.* **1995**, *117*, 6990−6993. (b) Dodsworth, E. S.; Vlcek, A. A.; Lever, A. B. P. *Inorg. Chem.* **1994**, *33*, 1045−1049.

(37) The impurity at 1.05 V in the SWV voltammogram (Figure 5b) is not responsible for the first appearance of the 712 nm. We equilibrated the spectrum at 1.20 V and only a small change at the 461 nm MLCT band was seen.

(38) (a) Kattnig, D. R.; Mladenova, B.; Grampp, G.; Kaiser, C.; Heckmann, A.; Lambert, C. *J. Phys. Chem. C* **2009**, *113*, 2983−2995.

(39) Ramirez, C. L.; Pegoraro, C.; Trupp, L.; Bruttomesso, A.; Amorebieta, V. T.; Vera, D. M. A.; Parise, A. R. *Phys. Chem. Chem. Phys.*, **2011**, *132*007620080.

(40) Low, P. J.; Paterson, M. A. J.; Goeta, A. E.; Yufit, D. S.; Howard, J. A. K.; Cherryman, J. C.; Tackleyb, R.; Brown, B. *J. Mater. Chem.* **2004**, *14*, 2516−2523.

(41) We could not follow the suggestion of Referee #1 regarding measuring the EPR spectrum of the dioxidized specie because we did not find a suitable chemical reagent for oxidation of **Ru-(dt3pya)$_2$** at 1.4 V.

(42) Nelson, R. F.; Fritsch, J. M.; Marcoux, L. S.; Donald, W.; Leedy, D. W.; Adams, R. N. *J. Am. Chem. Soc.* **1966**, *88*, 3498−3503.

(43) This is a very rough estimation of the diabatic distance because **dt3pya** is rotating, and redox centers are not at a fixed position. We estimate that separation between the central nitrogens of **dt3pya** span from 5 to 10 Å.

(44) Shin, Y. K.; Brunschwig, B. S.; Creutz, C.; Sutin, N. *J. Phys. Chem.* **1996**, *100*, 8157−8169.

(45) Lambert, C.; Nöll, G.; Schelter, J. *Nat. Mater.* **2002**, *1*, 69−73.

(46) Launay, J. P.; Coudret, C.; Hortholary, C. *J. Phys. Chem. B* **2007**, *111*, 6788−6797.

(47) Lin, B. C.; Cheng, C. P.; Lao, Z. P. M. J. *Phys. Chem. A* **2003**, *107* (26), 5241−5251.